Article

Highly Metallized Polymers: Synthesis, Characterization, and Lithographic Patterning of Polyferrocenylsilanes with Pendant Cobalt, Molybdenum, and Nickel Cluster Substituents

Wing Yan Chan, Scott B. Clendenning, Andrea Berenbaum, Alan J. Lough, Stephane Aouba, Harry E. Ruda, and Ian Manners

J. Am. Chem. Soc., **2005**, 127 (6), 1765-1772• DOI: 10.1021/ja045386i • Publication Date (Web): 21 January 2005

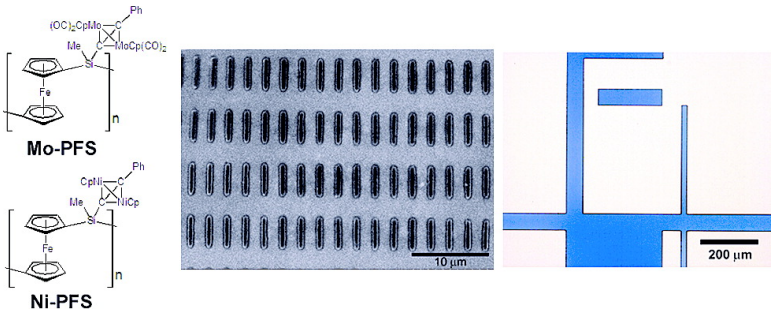

More About This Article

Additional resources and features associated with this article are available within the HTML version:

- Supporting Information
- Links to the 14 articles that cite this article, as of the time of this article download
- Access to high resolution figures
- Links to articles and content related to this article
- Copyright permission to reproduce figures and/or text from this article

View the Full Text HTML

J|A|C|S
ARTICLES
Published on Web 01/21/2005

Highly Metallized Polymers: Synthesis, Characterization, and Lithographic Patterning of Polyferrocenylsilanes with Pendant Cobalt, Molybdenum, and Nickel Cluster Substituents

Wing Yan Chan,[†] Scott B. Clendenning,[†,§] Andrea Berenbaum,[†] Alan J. Lough,[†] Stephane Aouba,[‡] Harry E. Ruda,[‡] and Ian Manners*[,†]

Contribution from the Department of Chemistry, University of Toronto, 80 St. George Street, Toronto, Ontario, Canada, M5S 3H6, and Centre for Advanced Nanotechnology, University of Toronto, Ontario, Canada, M5S 3E4

Received July 30, 2004; E-mail: imanners@chem.utoronto.ca

Abstract: High molecular weight, soluble, air- and moisture-stable, highly metallized (>25 wt% metal) polyferrocenylsilanes (PFS) $[Fe(\eta\text{-}C_5H_4)_2Si(Me)\{Co_2(CO)_6C_2Ph\}]_n$ (**Co**−**PFS**), $[Fe(\eta\text{-}C_5H_4)_2Si(Me)\{Mo_2Cp_2(CO)_4C_2Ph\}]_n$ (**Mo**−**PFS**), and $[Fe(\eta\text{-}C_5H_4)_2Si(Me)\{Ni_2Cp_2C_2Ph\}]_n$ (**Ni**−**PFS**) containing pendant cobalt, molybdenum, and nickel clusters, respectively, have been prepared via macromolecular clusterization of an acetylide-substituted PFS $[Fe(\eta\text{-}C_5H_4)_2Si(Me)C{\equiv}CPh]_n$ with $[Co_2(CO)_8]$, $[\{MoCp(CO)_2\}_2]$, or $[\{NiCp(CO)\}_2]$. The extent of clusterization achieved was in the range of 70−75%. All three highly metallized polymers were demonstrated to function as negative-tone resists in electron-beam lithography, while **Co**−**PFS** and **Mo**−**PFS** were successfully patterned by UV−photolithography, allowing the fabrication of micron-sized bars, dots, and lines. These studies suggest that the highly metallized polymers may be useful in the fabrication of patterned arrays of alloy nanoparticles for both materials science and catalytic applications.

Introduction

Metal-containing polymers are attracting growing attention as functional materials.[1−3] For example, the presence of transition metal centers in a polymer has enabled redox-control of the size and shape of a macroscopic object;[4] selective binding and sensing of small molecules, metal ions, and biomolecules;[5] the introduction of desirable photophysical properties;[6] and the generation of liquid crystallinity,[7] magnetic nanoparticle composites,[8] and catalytic[9] and supramolecular[10] materials. Notwithstanding the significant advances made in the metallopolymer area in the past decade, most materials reported to date still contain relatively low concentrations of metal atoms of limited variety, restricting the scope of both the field and potential applications.

Polymers containing substituents that can be transformed into metal clusters represent an excellent potential scaffold for the preparation of processible, highly metallized materials with intriguing properties.[11] Introduction of metal clusters into a polymer can dramatically increase its metal content, especially when the polynuclear moieties are present in every repeat unit. Several research groups have previously taken advantage of this

[†] Department of Chemistry.
[‡] Centre for Advanced Nanotechnology.
[§] Current address: Intel Corporation, Mail Stop AL3-62, 3585 SW 198th Avenue, Aloha, OR 97007.

(1) (a) Archer, R. D. *Inorganic and Organometallic Polymers*; John Wiley & Sons Inc.: New York, 2001. (b) Newkome, G. R.; He, E.; Moorefield, C. N. *Chem. Rev.* **1999**, *99*, 1689−1746. (c) Astruc, D.; Chardac, F. *Chem. Rev.* **2001**, *101*, 2991−3023.
(2) (a) Abd-El-Aziz, A. S., Ed. *Macromol. Symp.* **2003**, *196*, 1−353. (b) Abd-El-Aziz, A. S., Harvey, P. D., Eds. *Macromol. Symp.* **2004**, *209*, 1−251. (c) Kingsborough, R. P.; Swager, T. M. *Prog. Inorg. Chem.* **1999**, *48*, 123−231. (d) Wolf, M. O. *Adv. Mater.* **2001**, *13*, 545−553.
(3) (a) Manners, I. *Science* **2001**, *294*, 1664−1666. (b) Manners, I. *Synthetic Metal-Containing Polymers*; Wiley-VCH: Weinheim, Germany, 2004.
(4) (a) Yoshida, R.; Takahashi, T.; Yamaguchi, T.; Ichijo, H. *Adv. Mater.* **1997**, *9*, 175−178. (b) Arsenault, A. C.; Míguez, H.; Kitaev, V.; Ozin, G. A.; Manners, I. *Adv. Mater.* **2003**, *15*, 503−507.
(5) (a) Caruana, D. J.; Heller, A. *J. Am. Chem. Soc.* **1999**, *121*, 769−774. (b) Wang, Z.; McWilliams, A. R.; Evans, C. E. B.; Lu, X.; Chung, S.; Winnik, M. A.; Manners, I. *Adv. Funct. Mater.* **2002**, *12*, 415−419. (c) Albrecht, M.; van Koten, G. *Adv. Mater.* **1999**, *11*, 171−174. (d) Wang, B.; Wasielewski, M. R. *J. Am. Chem. Soc.* **1997**, *119*, 12−21.
(6) (a) Wong, W.-Y.; Liu, L.; Poon, S.-Y.; Choi, K.-H.; Cheah, K.-W.; Shi, J.-X. *Macromolecules* **2004**, *37*, 4496−4504. (b) Wong, C. T.; Chan, W. K. *Adv. Mater.* **1999**, *11*, 455−459. (c) Ley, K. D.; Ed Whittle, C.; Bartberger, M. D.; Schanze, K. S. *J. Am. Chem. Soc.* **1997**, *119*, 3423−3424.
(7) (a) Steffen, W.; Köhler, B.; Altmann, M.; Scherf, U.; Stitzer, K.; zur Loye, H.-C.; Bunz, U. H. F. *Chem.—Eur. J.* **2001**, *7*, 117−126. (b) Oriol, L.; Serrano, J. L. *Adv. Mater.* **1995**, *7*, 348−369. (c) Hagihara, N.; Sonogashira, K.; Takahashi, S. *Adv. Polym. Sci.* **1981**, *41*, 149−179. (d) Liu, X.-H.; Bruce, D. W.; Manners, I. *Chem. Commun.* **1997**, 289−290.
(8) (a) MacLachlan, M. J.; Ginzburg, M.; Coombs, N.; Coyle, T. W.; Raju, N. P.; Greedan, J. E.; Ozin, G. A.; Manners, I. *Science* **2000**, *287*, 1460−1463. (b) Temple, K.; Kulbaba, K.; Power-Billard, K. N.; Manners, I.; Leach, K. A.; Xu, T.; Russell, T. P.; Hawker, C. J. *Adv. Mater.* **2003**, *15*, 297−300.
(9) (a) Ajjou, A. N.; Alper, H. *J. Am. Chem. Soc.* **1998**, *120*, 1466−1468. (b) Peckham, T. J.; Nguyen, P.; Bourke, S. C.; Wang, Q.; Harrison, D. G.; Zoricak, P.; Russell, C.; Liable-Sands, L. M.; Rheingold, A. L.; Lough, A. J.; Manners, I. *Organometallics* **2001**, *20*, 3035−3043. (c) Köllner, C.; Pugin, B.; Togni, A. *J. Am. Chem. Soc.* **1998**, *120*, 10274−10275. (d) Hinderling, C.; Keles, Y.; Stöckli, T.; Knapp, H. F.; de los Arcos, T.; Oelhafen, P.; Korczagin, I.; Hempenius, M. A.; Vancso, G. J.; Pugin, R.; Heinzelmann, H. *Adv. Mater.* **2004**, *16*, 876−879. (e) Lastella, S.; Jung, Y. J.; Yang, H.; Vajtai, R.; Ajayan, P. M.; Ryu, C. Y.; Rider, D. A.; Manners, I. *J. Mater. Chem.* **2004**, 1791−1794.
(10) (a) Park, C.; McAlvin, J. E.; Fraser, C. L.; Thomas, E. L. *Chem. Mater.* **2002**, *14*, 1225−1230. (b) Wang, X.-S.; Arsenault, A.; Ozin, G. A.; Winnik, M. A.; Manners, I. *J. Am. Chem. Soc.* **2003**, *125*, 12686−12687. (c) Bender, J. L.; Corbin, P. S.; Fraser, C. L.; Metcalf, D. H.; Richardson, F. S.; Thomas, E. L.; Urbas, A. M. *J. Am. Chem. Soc.* **2002**, *124*, 8526−8527. (d) Beck, J. B.; Rowan, S. J. *J. Am. Chem. Soc.* **2003**, *125*, 13922−13923. (e) Eitouni, H. B.; Balsara, N. P. *J. Am. Chem. Soc.* **2004**, *126*, 7446−7447. (f) Lohmeijer, B. G. G.; Schubert, U. S. *Angew. Chem. Int. Ed.* **2002**, *41*, 3825−3829. (g) Chen, B.; Sleiman, H. F. *Macromolecules* **2004**, *37*, 5866−5872.

type of synthetic strategy to prepare polymers with pendant cluster substituents. For example, Han and co-workers reported an azulene−thiophene copolymer containing ruthenium carbonyl clusters of varying nuclearity ($Ru_x(CO)_y$ ($x = 2-4$)) coordinated to the azulene.[12] The metal content of the copolymer was tuned by varying the amount of $[Ru_3(CO)_{12}]$ used, resulting in half or complete metallization of the azulene units. Through radical copolymerization of cluster-containing monomers or macromolecular substitution of a copolymer with a metal cluster, Pomogailo and co-workers have synthesized a variety of cluster-containing copolymers with molybdenum, osmium, or rhodium clusters.[13] Allen and Bahadur have reported complexation of phenylethynyl substituents with $[Co_2(CO)_8]$ in a styrene copolymer containing phenylacetylide-substituted pendant cyclophosphazenes.[14] Several examples of metallopolymers with metal clusters in the backbone have also been reported. For example, Humphrey and co-workers synthesized a variety of oligourethanes using bimetallic Mo_2Ir_2 cluster diols and alkyl- or aryldiisocyanates, with typical degrees of polymerization between 5 and 8.[15] In addition, Johnson and co-workers prepared an electron-beam sensitive cluster polymer based on $[Ru_6C(CO)_{15}]$ as a precursor to ruthenium-based nanoparticle chains and conducting wires.[16] Also, Brook and co-workers reported that triple bonds in an oligo(alkynylsilane) can be complexed with $[Co_2(CO)_8]$ to give cobalt clusters along the oligomer backbone.[17] Besides linear polymers, metallodendrimers containing metal clusters at the core or on the surface of the dendrimer have also been synthesized.[18] However, despite all these advances, the concentration of cluster-containing moieties in virtually all of these materials is low. They are often separated by long organic spacers, and typical metal contents are less than 10 wt%.[19]

Recent research has shown that ring-opening polymerization (ROP) of strained metallocenophanes gives polymetallocenes that possess many interesting characteristics for materials science applications.[20] Although a polymetallocene contains only one metal atom per repeat unit, its metal content may be increased by judicious modifications of the bridging atom substituents of the metallocenophane. We have recently reported the synthesis of polyferrocenylsilanes (PFSs) **2** with acetylenic substituents through platinum-catalyzed ROP of strained, acetylide-substituted sila[1]ferrocenophanes.[21] These metallopolymers are potentially excellent precursors to highly metallized PFSs as the acetylenic substituents should react with a wide variety of metal complexes in macromolecular clusterization reactions.[22,23] In this paper, we report full details of the synthesis and characterization of highly metallized PFSs with pendant cobalt, molybdenum, and nickel clusters through macromolecular complexation of carbon−carbon triple bonds in acetylide-substituted PFSs. We also discuss preliminary studies of the materials science applications of these highly metallized polymers as resists in electron-beam lithography and UV−photolithography.

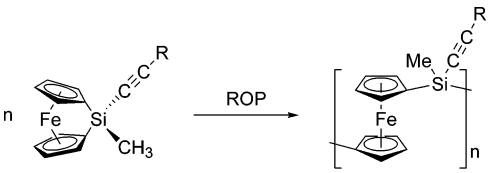

1a (R = Ph)
1b (R = ^{n}Bu)

2a (R = Ph)
2b (R = ^{n}Bu)

Results and Discussion

To develop a general route to highly metallized PFSs, we explored macromolecular clusterization of carbon−carbon triple bonds in acetylide-substituted PFSs **2** using cobalt, molybdenum, and nickel complexes. The use of dinuclear metal complexes was anticipated to increase the number of metal atoms in each polymer repeat unit from one to three.

Synthesis and Characterization of Polyferrocenylsilanes with Pendant Organocobalt Clusters (3a and 3b). We began our studies with $[Co_2(CO)_8]$ since it reacts with alkynes under very mild reaction conditions.[24] Acetylide-substituted PFSs **2a** and **2b** were synthesized via platinum-catalyzed ROP of strained sila[1]ferrocenophanes **1a** and **1b**, respectively; triethylsilane was used as a capping agent to control molecular weight and thereby promote polymer solubility.[25] The acetylide-substituted PFSs readily reacted with excess $[Co_2(CO)_8]$ at 25 °C to give

(11) (a) Braunstein, P., Oro, L. A., Raithby, P. R., Eds. *Metal Clusters in Chemistry*; VCH Publishers Inc.: New York, 1999. (b) Adams, R. D., Cotton, F. A., Eds. *Catalysis by Di- and Polynuclear Metal Cluster Complexes*; Wiley-VCH: New York, 1998. (c) Moskovits, M., Ed. *Metal Clusters*; John Wiley & Sons: New York, 1986. (d) Johnson, B. F. G., Ed. *Transition Metal Clusters*; John Wiley & Sons: Chichester, U.K., 1980. (e) Gates, B. C., Guczi, L., Knözinger, H., Eds. *Metal Clusters in Catalysis*; Elsevier: Amsterdam, 1986.

(12) Wang, F.; Lai, Y.-H.; Han, M. Y. *Org. Lett.* **2003**, *5*, 4791−4794.

(13) (a) For Mo cluster copolymers, see: Golubeva, N. D.; Adamenko, O. A.; Boiko, G. N.; Petrova, L. A.; Ol'khov, Y. A.; Pomogailo, A. D. *Inorg. Mater.* **2004**, *40*, 363−371. (b) For Os cluster copolymers, see: Bravaya, N. M.; Pomogailo, A. D.; Maksakov, V. A.; Kirin, V. P.; Grachev, V. P.; Kuzaev, A. I. *Russ. Chem. Bull.* **1995**, *44*, 1062−1067. (c) For Rh cluster copolymers, see: Lyakhovich, A. M.; Mikhailova, S. S.; Pomogailo, S. I.; Dzhardimalieva, G. I.; Pomogailo, A. D. *Macromol. Symp.* **2003**, *204*, 251−256.

(14) Allen, C. W.; Bahadur, M. *J. Inorg. Organomet. Polym.* **1998**, *8*, 23−31.

(15) Lucas, N. T.; Humphrey, M. G.; Rae, A. D. *Macromolecules* **2001**, *34*, 6188−6195.

(16) Johnson, B. F. G.; Sanderson, K. M.; Shephard, D. S.; Ozkaya, D.; Zhou, W.; Ahmed, H.; Thomas, M. D. R.; Gladden, L.; Mantle, M. *Chem. Commun.* **2000**, 1317−1318.

(17) Kuhnen, T.; Stradiotto, M.; Ruffolo, R.; Ulbrich, D.; McGlinchey, M. J.; Brook, M. A. *Organometallics* **1997**, *16*, 5048−5057.

(18) (a) Wang and Zheng reported a metal cluster-based dendrimer containing the hexanuclear $[Re_6Se_8]^{2+}$ core with physical properties highly dependent on the structure of the organic dendrons used: Wang, R.; Zheng, Z. *J. Am. Chem. Soc.* **1999**, *121*, 3549−3550. (b) Seyferth and co-workers prepared two carbosilane metallodendrimers via complexation of an ethynyl substituent of peripheral silicon atoms with $[Co_2(CO)_8]$ to give cobalt clusters: Seyferth, D.; Kugita, T.; Rheingold, A. L.; Yap, G. P. A. *Organometallics* **1995**, *14*, 5362−5366.

(19) (a) Rare exceptions to this are rhodium cluster-containing polymers in ref 13c (maximum 12.7 wt% Rh), Mo_2Ir_2 cluster oligourethanes in ref 15 (maximum 54 wt% metal), and the $Ru_6C(CO)_{15}$ cluster polymer in ref 16 (44 wt% Ru). (b) Recently, examples of well-defined block copolymers containing cobalt cluster substituents have been reported: Mîinea, L. A.; Sessions, L. B.; Ericson, K. D.; Glueck, D. S.; Grubbs, R. B. *Macromolecules* **2004**, *37*, 8967−8972. (c) Häussler, M.; Zheng, R.; Lam, J. W. Y.; Tong, H.; Dong, H.; Tang, B. Z. *J. Phys. Chem. B* **2004**, *108*, 10645−10650.

(20) (a) Manners, I. *Chem. Commun.* **1999**, 857−865. (b) Kulbaba, K.; Manners, I. *Macromol. Rapid Commun.* **2001**, *22*, 711−724.

(21) Berenbaum, A.; Lough, A. J.; Manners, I. *Organometallics* **2002**, *21*, 4415−4424.

(22) For a brief communication reporting the synthesis of **Co−PFS**, see: Berenbaum, A.; Ginzburg-Margau, M.; Coombs, N.; Lough, A. J.; Safa-Sefat, A.; Greedan, J. E.; Ozin, G. A.; Manners, I. *Adv. Mater.* **2003**, *15*, 51−55.

(23) For general reviews on metal cluster formation from carbon−carbon triple bonds, see: (a) Melikyan, G. G.; Nicholas, K. M. In *Modern Acetylene Chemistry*; Stang, P. J., Diederich, F., Eds.; VCH: Weinheim, Germany, 1995; pp 99−138. (b) Sappa, E. *J. Organomet. Chem.* **1999**, *573*, 139−155. (c) Deabate, S.; Giordano, R.; Sappa, E. *J. Cluster Sci.* **1997**, *8*, 407−459. (d) Sappa, E.; Tiripicchio, A.; Braunstein, P. *Chem. Rev.* **1983**, *83*, 203−239.

(24) Nicholas, K. M.; Nestle, M. O.; Seyferth, D. In *Transition Metal Organometallics in Organic Synthesis*; Alper, H., Ed.; Academic: New York, 1978; Vol. 2, pp 2−63.

(25) We have previously demonstrated the use of Et_3SiH for molecular weight control in Pt-catalyzed ROP of $Fe(\eta\text{-}C_5H_4)_2SiMe_2$: Gómez-Elipe, P.; Resendes, R.; Macdonald, P. M.; Manners, I. *J. Am. Chem. Soc.* **1998**, *120*, 8348−8356.

Scheme 1. Reaction of **2a** and **2b** with $[Co_2(CO)_8]$ and Synthesis of **Co−PFS 3a** and **3b**

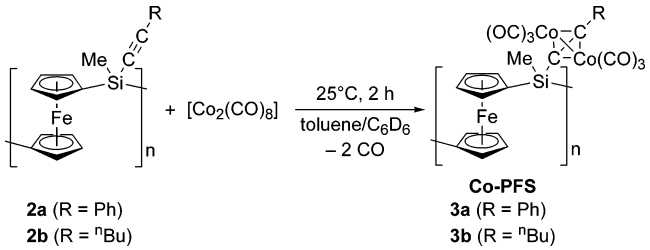

cobalt clusters at the triple bond (Scheme 1). After precipitation into hexanes, the air- and moisture-stable cobalt-clusterized PFSs (**Co−PFSs**) **3a** and **3b** were isolated as dark brown solids in 91 and 64% yield, respectively.

Analysis of **Co−PFS 3a** by ^{1}H NMR spectroscopy showed that ca. 75% of the carbon−carbon triple bonds in PFS **2a** were clusterized. The ratio of clusterized units to unclusterized units was calculated using the integrals of the methyl resonances for these units. The ^{1}H NMR spectrum of **3a** contained a broad singlet at $\delta = 1.12$ ppm for methyl protons in a cobalt-containing polymer repeat unit, shifted downfield from that of **2a** ($\delta = 0.81$ ppm).[21] A downfield shift of the methyl resonance and broadening of the signals upon clusterization are common features of the highly metallized polymers in this work. The resonance for the methyl group in a polymer repeat unit without cobalt clusters was found at $\delta = 0.73$ ppm. The ^{13}C{^{1}H} NMR spectrum of **3a** showed a resonance at $\delta = 71.0$ ppm for the *ipso*-Cp carbons, again shifted downfield from those in **2a** ($\delta = 69.0$ ppm).[21] The solid-state ^{29}Si{^{1}H} NMR spectrum of **3a** showed two singlets at $\delta = -5.6$ and -23.1 ppm for repeat units with and without cobalt clusters, respectively. Analysis of the IR spectrum of **3a** showed that all carbonyl ligands were terminal. The molecular weight of **Co−PFS 3a** could not be determined using gel permeation chromatography (GPC) as the polymer interacted very strongly with the styragel column and did not elute. In a control experiment, $[Fe(\eta\text{-}C_5H_4)_2SiMe_2]_n$ (a PFS with no clusterizable substituents) was treated with $[Co_2(CO)_8]$ as described for the synthesis of **Co−PFS 3a**. GPC analysis of the resulting polymer showed no significant decrease in M_w, so we assume that $[Co_2(CO)_8]$ does not cause significant chain cleavage in PFS **2a**.[26] For **Co−PFS 3b**, spectroscopic data were also consistent with clusterization of the triple bond in PFS **2b**. Analysis of the ^{1}H NMR spectrum of **Co−PFS 3b** gave an extent of clusterization of ca. 75%. As for the case of **Co−PFS 3a**, the ratio of clusterized units to unclusterized units in **Co−PFS 3b** was calculated using the integrals of the methyl resonances for these units.

Synthesis and Characterization of a Polyferrocenylsilane with Pendant Organomolybdenum Clusters (4). Molybdenum-clusterized PFS (**Mo−PFS**) **4** was synthesized from acetylide-substituted PFS **2a** ($M_w = 2.4 \times 10^5$, PDI = 2.26) using $[\{MoCp(CO)_2\}_2]$ as the metal source (Scheme 2). Precipitation of the reaction mixture into methanol gave the highly metallized polymer as an air- and moisture-stable dark brown solid in 49% yield. Analysis by ^{1}H NMR spectroscopy showed that ca. 69% of triple bonds were clusterized, as determined by the integration

(26) In addition, treatment of the strained monomer **1a** with $[Co_2(CO)_8]$ leads to quantitative clusterization without inducing any ring-cleavage chemistry (see ref 28). This also strongly supports the assertion that there is minimal chain cleavage when PFS **2a** and **2b** are treated with $[Co_2(CO)_8]$.

Scheme 2. Reaction of **2a** with $[\{MoCp(CO)_2\}_2]$ and Synthesis of **Mo−PFS 4**

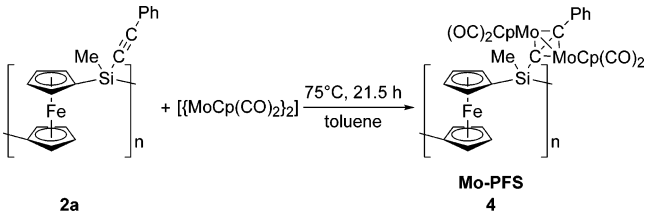

Scheme 3. Photolysis of **1a** with $[\{NiCp(CO)\}_2]$ and Synthesis of **5**

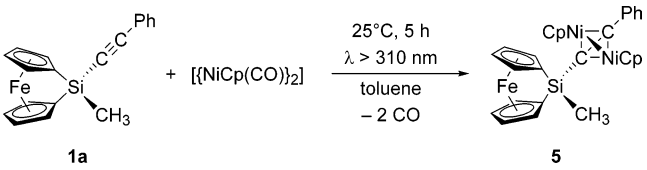

of methyl resonances for the clusterized and unclusterized repeat units. The methyl resonance for a molybdenum-clusterized polymer repeat unit in **4** was found as a multiplet at $\delta = 1.29-1.20$ ppm in the ^{1}H NMR spectrum. The resonance for the Cp protons of the molybdenum cluster was found at $\delta = 5.04$ ppm. The ^{13}C{^{1}H} NMR spectrum of **4** showed a singlet for the Cp ring bound to molybdenum at $\delta = 93.5$ ppm, and the resonance for *ipso*-Cp carbons was found at $\delta = 69.7$ ppm. The solid-state ^{29}Si{^{1}H} NMR spectrum of **4** contained two singlets at $\delta = 0.4$ and -22.9 ppm, corresponding to silicon atoms in a polymer repeat unit with and without molybdenum clusters, respectively. Infrared spectroscopy revealed the presence of a semibridging carbonyl ligand in **Mo−PFS 4**, typical for molybdenum−alkyne complexes of this kind.[27,28] GPC analysis of **Mo−PFS 4** gave $M_w = 5.4 \times 10^5$ and PDI = 1.49; a molecular weight increase upon clusterization of PFS **2a** is consistent with the incorporation of molybdenum clusters within the polymer.

Synthesis and Characterization of a Sila[1]ferrocenophane and a Polyferrocenylsilane Containing Pendant Organonickel Clusters (5 and 6). Using $[Ni(cod)_2]$ as the metal source, we have recently synthesized a sila[1]ferrocenophane containing a pendant organonickel unit with a bis(diphenylphosphino)-ethane ligand.[28,29] However, only one nickel atom was introduced at the alkyne, possibly due to steric reasons. Since our goal was to prepare highly metallized PFS with two metal atoms bound to the alkyne ligand, we aimed to incorporate a cluster of two nickel atoms bound to each other through a metal−metal bond. The complex $[\{NiCp(CO)\}_2]$ has been shown to react with alkynes to give the clusters $[Cp_2Ni_2(RC_2R')]$ in thermal and photochemical reactions.[30] To obtain structural information and coordination geometry of the alkyne in our system, we synthesized a model monomer from $[\{NiCp(CO)\}_2]$ and acetylide-substituted monomer **1a**. After irradiating the solution of **1a** and $[\{NiCp(CO)\}_2]$ with a mercury lamp ($\lambda > 310$ nm, Scheme 3) for 5 h, 90% of the monomer was clusterized. Nickel-

(27) Bailey, W. I., Jr.; Chisholm, M. H.; Cotton, F. A.; Rankel, L. A. *J. Am. Chem. Soc.* **1978**, *100*, 5764−5773.
(28) Chan, W. Y.; Berenbaum, A.; Clendenning, S. B.; Lough, A. J.; Manners, I. *Organometallics* **2003**, *22*, 3796−3808.
(29) We were unable to induce ROP of highly metallized sila[1]ferrocenophanes containing Co, Mo, or Ni. A variety of experimental conditions were attempted: thermal, heating at 95 °C overnight (^{1}H NMR showed no conversion); transition metal catalysis, no polymer formation (by ^{1}H NMR) with Karstedt's catalyst, $PtCl_2$ or $Rh(cod)_2OTf$ at 25 or 50 °C; anionic, catalytic amounts of BuLi caused declusterization.
(30) Forbes, E. J.; Iranpoor, N. *J. Organomet. Chem.* **1982**, *236*, 403−407.

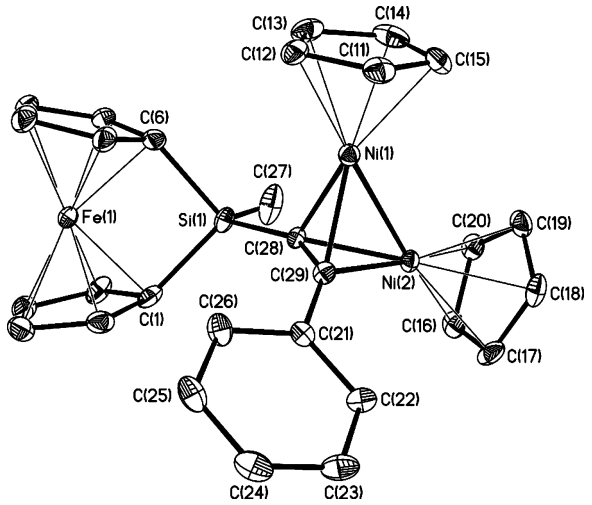

Figure 1. Molecular structure of **5** (thermal ellipsoids at 30% probability). Hydrogen atoms have been removed for clarity. Selected bond lengths (Å) and bond angles (deg): Fe(1)−Si(1) 2.7143(12), Ni(1)−Ni(2) 2.3379(6), C(28)−C(29) 1.342(6), α 21.21(21), C(1)−Si(1)−C(6) 95.63(18), Si(1)−C(28)−C(29) 154.0(3), C(28)−C(29)−C(21) 143.6(4).

clusterized monomer **5** was isolated as a dark green solid after recrystallization from a toluene/hexanes (3:2) solution in 44% yield.

The ^{1}H NMR spectrum of **5** showed a singlet at $\delta = 5.23$ ppm for the Cp protons in the nickel cluster, shifted downfield from [{NiCp(CO)}$_2$] ($\delta = 5.15$ ppm). The methyl proton resonance of the monomer was also shifted downfield to $\delta = 0.81$ ppm upon clusterization of the carbon−carbon triple bond (cf. **1a**: $\delta = 0.61$ ppm).[21] The ^{13}C{^{1}H} NMR spectrum of **5** contained a resonance at $\delta = 87.9$ ppm for Cp carbons bound to nickel, and the resonance for the *ipso*-Cp carbons was found at $\delta = 34.7$ ppm. The ^{29}Si{^{1}H} NMR spectrum of **5** contained a singlet at $\delta = -18.1$ ppm, shifted downfield from that of **1a** ($\delta = -27.8$ ppm).[21]

The molecular structure of **5** was further confirmed by single-crystal X-ray crystallography (Figure 1). The tilt angle between the Cp planes (α) in **5** was 21.21(21)°, which is comparable to sila[1]ferrocenophanes with pendant cobalt or molybdenum clusters (ca. 19−21°).[28] The Ni−Ni bond in **5** was orthogonal to the acetylenic bond, as observed in the analogous complex [$Cp_2Ni_2(PhC_2Ph)$].[31] The Ni−Ni bond length in **5** is 2.3379(6) Å and is typical for nickel−alkyne complexes.[31,32] Upon coordination, the acetylenic bond lengthened significantly from 1.197(4)[21] to 1.342(6) Å, which is slightly longer than that of free ethylene (d(C=C) = 1.34 Å).[33] Angles around the acetylenic carbons range from 143 to 154°, indicating a bending back of the phenyl group upon clusterization of the alkyne.

After confirming the structure of the model nickel species, we proceeded to synthesize nickel-clusterized PFS (**Ni−PFS**) **6**.[29] To access lower molecular weight PFS **2a** for clusterization, we used a more active silane, $ClPh_2SiH$, for molecular weight control.[34] We prepared **Ni−PFS 6** through macromolecular clusterization of PFS **2a** ($M_n = 4700$, PDI = 2.57) with [{NiCp(CO)}$_2$] (Scheme 4). Precipitation into hexanes gave the air- and moisture-stable **Ni−PFS 6** as a green powder in 73% yield. As anticipated, the polymer remained very soluble in common organic solvents, such as THF and toluene. The ^{1}H NMR spectrum of **6** showed broad peaks at $\delta = 7.84-7.58$ and 7.32−6.96 ppm for phenyl protons, and the resonance for Cp protons in the nickel cluster was found at $\delta = 5.20$ ppm. Analysis of the methyl resonances showed that ca. 75% of triple bonds were clusterized.[35] As for the cases of the other cluster polymers, the ratio of clusterized units to unclusterized units was calculated using the integrals of the methyl resonances. The ^{13}C{^{1}H} NMR spectrum of **6** showed a singlet at $\delta = 88.0$ ppm for Cp carbons bound to nickel. The resonance for the *ipso*-Cp carbons in the nickel-containing unit was found at $\delta = 68.9$ ppm; the corresponding resonance for a repeat unit lacking nickel was too broad and could not be discerned from the baseline. The ^{29}Si{^{1}H} NMR spectrum of **6** contained a singlet at $\delta = -13.2$ ppm. The resonance for silicon atoms in repeat units with no nickel clusters was not detected. GPC analysis of **Ni−PFS 6** gave $M_n = 7100$ and PDI = 1.91; the increase in molecular weight after clusterization is consistent with the incorporation of nickel clusters in the polymer.

Scheme 4. Photolysis of **2a** with [{NiCp(CO)$_2$}] and Synthesis of **Ni−PFS 6**

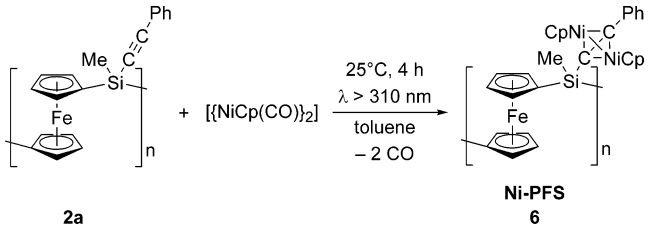

Lithographic Patterning of Highly Metallized PFSs. PFS materials with low metal contents have previously been used to fabricate iron-containing nanostructures which are of interest with respect to their magnetic, etch-resistant, and catalytic properties.[9d,e,36] Highly metallized polymers are even more promising precursors to dense arrays of metallic nanostructures via thermal or plasma treatment, and the resulting nanostructures may find applications as a result of their physical and catalytic properties. For many applications (e.g., in spintronic devices), convenient methods of patterning the materials are necessary to provide ultimate control over the spatial distribution of nanoparticles. We have previously reported preliminary details on the lithographic patterning of **Co−PFS 3a** using electron-beam lithography[37] and UV−photolithography,[38] as well as thermal and plasma treatment[39] to generate arrays of magnetic

(31) Mills, O. S.; Shaw, B. W. *J. Organomet. Chem.* **1968**, *11*, 595−600.
(32) (a) For [$Cp_2Ni_2(HC_2H)$], see: Wang, Y.; Coppens, P. *Inorg. Chem.* **1976**, *15*, 1122−1127. (b) For [$Cp_2Ni_2(CF_3C_2P(O)PPh_2)$], see: Restivo, R. J.; Ferguson, G.; Ng, T. W.; Carty, A. J. *Inorg. Chem.* **1977**, *16*, 172−176.
(33) Elschenbroich, C.; Salzer, A. *Organometallics: A Concise Introduction*; VCH Publishers Inc.: New York, 1992.
(34) Bartole-Scott, A.; Resendes, R.; Manners, I. *Macromol. Chem. Phys.* **2003**, *204*, 1259−1268.
(35) Although complete clusterization of the triple bonds in PFS **2a** was achieved in a very small scale reaction (15 mg **2a** in an NMR tube), we were unable to obtain greater than ca. 75% clusterization when the reaction was performed on a preparative scale. We attribute this to increased absorption of the incident light as the solution darkens, reducing the amount of light available to activate [{NiCp(CO)}$_2$].
(36) (a) Lammertink, R. G. H.; Hempenius, M. A.; Chan, V. Z.-H.; Thomas, E. L.; Vancso, G. J. *Chem. Mater.* **2001**, *13*, 429−434. (b) Massey, J. A.; Winnik, M. A.; Manners, I.; Chan, V. Z.-H.; Ostermann, J. M.; Enchelmaier, R.; Spatz, J. P.; Möller, M. *J. Am. Chem. Soc.* **2001**, *123*, 3147−3148.
(37) Clendenning, S. B.; Aouba, S.; Rayat, M. S.; Grozea, D.; Sorge, J. B.; Brodersen, P. M.; Sodhi, R. N. S.; Lu, Z.-H.; Yip, C. M.; Freeman, M. R.; Ruda, H. E.; Manners, I. *Adv. Mater.* **2004**, *16*, 215−219.
(38) Cheng, A. Y.; Clendenning, S. B.; Yang, G.; Lu, Z.-H.; Yip, C. M.; Manners, I. *Chem. Commun.* **2004**, 780−781.
(39) (a) Clendenning, S. B.; Han, S.; Coombs, N.; Paquet, C.; Rayat, M. S.; Grozea, D.; Brodersen, P. M.; Sodhi, R. N. S.; Yip, C. M.; Lu, Z.-H.; Manners, I. *Adv. Mater.* **2004**, *16*, 291−296. (b) Clendenning, S. B.; Manners, I. *J. Vac. Sci. Tech. B* **2004**, *22*, 3493−3496.

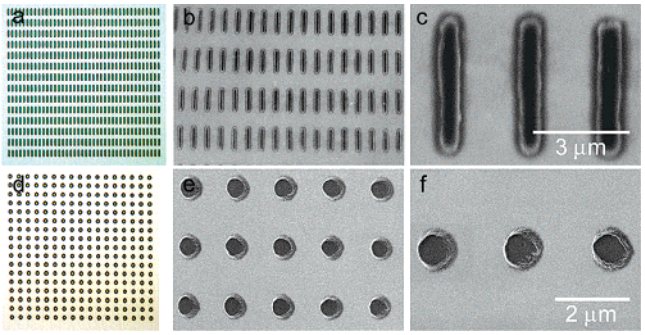

Figure 2. (a) Optical micrograph and (b and c) scanning electron micrographs of **Mo−PFS 4** microbars (0.5 × 4.0 μm^2), (d) optical micrograph, and (e and f) scanning electron micrographs of **Ni−PFS 6** microdots (diameter = 1.0 μm). Images (e) and (f) were acquired with a 33° stage tilt.

Fe/Co alloy nanoparticles. With the new highly metallized materials, **Mo−PFS 4** and **Ni−PFS 6**, in hand, we report here initial studies of their uses as lithographic resists.[40]

Electron-Beam Lithography (EBL). The direct-writing of metallic structures on metallopolymer resists using electron-beam lithography (EBL) is an attractive approach to nanofabrication.[41] Resists with high metal contents may permit the manufacture of magnetic metal structures either in one step or after pyrolytic treatment. The resulting metal nanoparticles may also have interesting potential uses in catalysis and spintronics. To fabricate functional devices from the highly metallized PFSs in this work,[42] we need to control the composition of the metal nanoparticle precursors. This can be achieved through varying the extent and type of clusterization in the polymers. Moreover, device fabrication necessitates precise control over spatial distribution of the metal nanoparticles.

Currently, there are very few studies that use metallopolymers as direct-write resists for metallic nanostructures. Johnson and co-workers briefly reported the use of a highly metallized polymer, $[Ru_6C(CO)_{15}(Ph_2PC_2PPh_2)]_n$, as a negative e-beam resist to fabricate conducting chains of nonmagnetic ruthenium nanoparticles down to 100 nm in width.[16] We have also disclosed in a recent communication that **Co−PFS 3a** can be used as a negative resist in EBL to fabricate microbars, dots, and curved lines.[37] With the new materials, **Mo−PFS 4** and **Ni−PFS 6**, we are interested in testing their ability to function as EBL resists and ultimately as precursors to metal nanoparticles.

A thin film of **Mo−PFS 4** (ca. 215 nm) was spin-coated onto a silicon substrate and exposed to an electron beam in a converted thermionic DSM 940 (Zeiss) scanning electron microscope. Various electron-beam doses between 5 and 25 mC/cm^2 were tested, a dose of 25 mC/cm^2 was optimal for obtaining uniformly patterned features and sufficient adhesion to the substrate following development in THF. Figure 2a−c shows optical and scanning electron micrographs of an array of 560 electron-beam fashioned bars (ca. 0.5 × 4.0 μm^2) after development by sonication in THF.[43] Clearly, the unexposed polymer was completely removed during development, indicating that

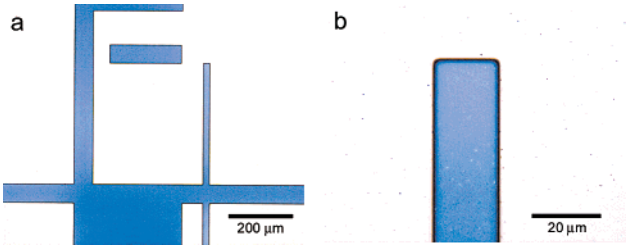

Figure 3. Bright field optical micrographs of (a) a pattern of **Mo−PFS 4** fabricated with UV−photolithography using a chrome contact mask; (b) the smallest line in (a) at higher magnification.

Mo−PFS 4 acts as a negative resist in EBL. As molybdenum−iron alloy nanoparticles are catalysts for single-walled carbon nanotube growth,[44] we are currently investigating the pyrolysis of these microbars to form patterned ceramics.

Ni−PFS 6 was also patterned by EBL as a negative resist. A dose study carried out on a thin film of **Ni−PFS 6** (ca. 193 nm) revealed that 20 mC/cm^2 was sufficient to give well-formed features with good adhesion to the substrate. Figure 2d−f shows optical and scanning electron micrographs of an array of 289 dots ca. 1.0 μm in diameter.[43] We are currently investigating the pyrolysis of these dot arrays to give nickel−iron alloy nanoparticles and their use as catalysts for carbon nanotube growth.[45]

UV−Photolithography. Photolithography is routinely used in the microelectronics industry for parallel patterning over large areas. Using a metallopolymer resist, it may be possible to pattern surfaces with metal-containing structures for device fabrication. Recently, we reported in a communication that a thin film of **Co−PFS 3a** acts as a negative-tone photoresist to give well-defined micron-sized features on a silicon substrate.[38] We are also interested in using **Mo−PFS 4** and **Ni−PFS 6** as resists in UV−photolithography. After a thin film of **Mo−PFS 4** on a silicon substrate was exposed to UV light (λ = 350−400 nm) through a chrome contact mask for 6 min, development in THF gave sharp features (20 μm and above) and completely removed any unexposed polymer (Figure 3). Lines in the pattern showed excellent shape retention and well-defined corners. As observed previously for **Co−PFS 3a**, **Mo−PFS 4** behaved as a negative-tone photoresist. We postulate that decarbonylation of the clusters during irradiation results in cross-linking of the polymer, making the exposed areas insoluble in THF. When we treated thin films of the parent unclusterized PFS **2a** and **Ni−PFS 6** under the same conditions, no pattern was observed after exposure, and all polymer was removed from the silicon substrate after development. Since neither PFS **2a** nor **Ni−PFS 6** contain carbonyl ligands, their inability to act as photoresists supports our postulate that decarbonylation is required to reduce the solubility of the UV-exposed polymer. Investigations are underway to determine and compare the resolutions of **Co−PFS 3a** and **Mo−PFS 4** as photoresists.[40]

Summary

We have successfully synthesized highly metallized PFSs **Co−PFS 3**, **Mo−PFS 4**, and **Ni−PFS 6** via macromolecular

(40) Although electron-beam lithography and UV−photolithography can be routinely used to generate structures down to ca. 50 and ca. 100 nm, respectively, no attempts were made to maximize the resolution of the feature sizes here.
(41) Gonsalves, K. E.; Merhari, L.; Wu, H.; Hu, Y. *Adv. Mater.* **2001**, *13*, 703−714.
(42) Theoretical calculations by M. B. A. Jalil indicated that a nanogranular-in-gap structure can be used as a magnetic field-controlled nanoswitch: Jalil, M. B. A. *IEEE Trans. Magn.* **2002**, *38*, 2613−2615.
(43) In the SEM images, the lighter areas around the microbars and microdots are due to charging artifacts on edges.
(44) Li, Y.; Liu, J.; Wang, Y.; Wang, Z. L. *Chem. Mater.* **2001**, *13*, 1008−1014.
(45) Using ethylene as the carbon source, Qian and co-workers have demonstrated that iron−nickel catalysts on alumina give helical carbon nanotubes: Qian, W.; Liu, T.; Wang, Z.; Yu, H.; Li, Z.; Wei, F.; Luo, G. *Carbon* **2003**, *41*, 2487−2493.

clusterization of carbon−carbon triple bonds in an acetylide-substituted PFS with the appropriate organometallic precursor. These readily prepared, highly metallized polymers are air- and moisture-stable and contain three metal atoms in at least 70% of polymer repeat units, with metal contents greater than 25 wt%. The molecular weight and metal content in this system can be controlled by varying the chain length of the parent acetylide-substituted PFS or by changing the extent of clusterization, respectively. This versatile synthetic approach should allow access to trimetallic polymers through sequential addition of two different metal complexes.

Co−PFS 3a, **Mo−PFS 4**, and **Ni−PFS 6** are interesting potential precursors to metallic nanoparticles with useful physical and catalytic properties. All three polymers function as negative-tone resists in electron-beam lithography to give well-formed microbars and/or microdots. **Co−PFS 3a** and **Mo−PFS 4** are good photoresists for UV−photolithography, giving sharp micron-sized features after UV exposure. **Ni−PFS 6** did not act as a photoresist under our experimental conditions; its lack of carbonyl ligands prevents decarbonylation and cross-linking of the polymer, which is a probable cause of the reduced solubility of exposed areas in **Co−PFS 3a** and **Mo−PFS 4**.

We are currently exploring pyrolytic and plasma treatments of these highly metallized PFSs. The resulting bimetallic iron-containing alloys should exhibit different magnetic properties as the identity of the second metal is varied. We anticipate that these metallic nanoparticles may have useful applications in catalysis and spintronic devices. Our results in these areas will be the subjects of future publications.

Experimental Section

[{NiCp(CO)}$_2$] and $ClPh_2SiH$ were purchased from Aldrich. [{NiCp(CO)}$_2$] was sublimed, and $ClPh_2SiH$ was distilled before use. [$Co_2(CO)_8$] and [{MoCp(CO)$_3$}$_2$] were purchased from STREM, and [$Co_2(CO)_8$] was sublimed immediately before use. Reactions involving [$Co_2(CO)_8$] require ambient light to proceed. Karstedt's catalyst (platinum−divinyltetramethyldisiloxane complex, 2.1−2.4 wt% Pt in xylenes) was purchased from Gelest and used as received. Compounds **1a**,[21] **1b**,[21] **2a**,[21] **2b**,[21] [Fe(η-C_5H_4)$_2$SiMe$_2$]$_n$,[25] and [MoCp(CO)$_2$]$_2$[46] were synthesized according to literature procedures.

Most reactions and manipulations were performed under an atmosphere of prepurified N_2 using Schlenk techniques or in an inert atmosphere glovebox. Unless specified as ACS grade, solvents were dried using the Grubbs method[47] or standard methods followed by distillation. The air- and moisture-stable polymers, **3a**, **3b**, **4**, and **6**, were handled in air with ACS grade solvents after workup. ^{1}H (300 MHz) NMR spectra were recorded on a Varian Gemini 300 or a Varian Mercury 300 spectrometer. ^{1}H (400 MHz), ^{13}C (100.5 MHz), and ^{29}Si (79.4 MHz) NMR spectra were recorded on a Varian Unity 400 spectrometer. ^{1}H resonances were referenced internally to the residual protonated solvent resonances. ^{13}C resonances were referenced internally to the deuterated solvent resonances. ^{29}Si NMR resonances were referenced externally to TMS. Solid-state ^{29}Si NMR spectra (CP/MAS) were recorded at 79.5 MHz on a Bruker DSX 400 spectrometer, with Si(SiMe$_3$)$_4$ (−9.9 ppm referenced to TMS) as an external chemical shift reference. Molecular weights were determined by gel permeation chromatography (GPC) using a Viscotek GPC MAX liquid chromatograph equipped with a Viscotek Triple Detector Array. The triple detector array consists of a deflection refractometer, a four-capillary differential viscometer, and a right angle laser light scattering detector (λ_0 = 670 nm). For PFS homopolymers, it has been shown that there is excellent agreement between M_w obtained from GPC with triple detection and absolute M_w obtained from low angle laser light scattering.[48] Conventional calibration was also used, and molecular weights were determined relative to polystyrene standards purchased from American Polymer Standards. In both cases, a flow rate of 1.0 mL/min was used with ACS grade THF as the eluent. Mass spectra were obtained with a VG 70−250S mass spectrometer in electron impact (EI) mode. The calculated isotopic distribution for each ion was in agreement with experimental values. Ultraviolet−visible spectra were recorded using a Perkin Elmer Lambda 900 UV−vis−NIR spectrometer. Elemental analyses were performed using a Perkin Elmer 2400 C/H/N analyzer. Photolysis of **1a** and **2a** was performed with a Philips 125 W high-pressure mercury-arc lamp. A Pyrex filter was placed inside the quartz immersion well to filter out wavelengths below 310 nm.

Synthesis of PFS 2a and 2b. PFS **2a** and **2b** were synthesized through Pt-catalyzed ROP of monomer **1a** and **1b**, respectively, using either Et_3SiH or $ClPh_2SiH$ for molecular weight control. A representative procedure using $ClPh_2SiH$ is given below. **1a** (1.00 g, 3.05 mmol) was dissolved in toluene (20 mL) to give a red solution. $ClPh_2SiH$ (0.15 mL, 0.77 mmol) and Karstedt's catalyst (100 μL) were sequentially added. The solution was stirred at 25 °C for 1 h, during which time the color became orange. Precipitation into rapidly stirred MeOH (100 mL) via a filter cannula gave an orange solid. After the precipitate was washed once with MeOH (30 mL) and once with ACS grade MeOH (30 mL), the solid was dried in vacuo to give an amber powder, with a yield of 1.00 g (90%). This polymer will be referred to as $OMePh_2Si$-capped **2a**; its ^{1}H NMR spectrum is consistent with that of previously reported high molecular weight **2a**.[21] GPC (conventional calibration) M_n = 4700, M_w = 12 100, PDI = 2.57.

Synthesis of Co−PFS 3a. In a typical reaction, [$Co_2(CO)_8$] (0.21 g, 0.61 mmol) in toluene (ca. 5 mL) was added to a solution of **2a** (0.10 g, 0.30 mmol, $M_n = 6.49 \times 10^4$, PDI = 1.9) in toluene (ca. 5 mL) at 25 °C. The reaction mixture was stirred for a further 2 h. The solution changed from light orange to dark brown, and the release of gas was noted. The solution was precipitated into hexanes through glass wool to remove small amounts of insoluble impurities, and the dark brown precipitate was washed three times with hexanes. All residual solvent was removed under high vacuum, leaving the dark brown powder **3a**, with a yield of 0.15 g (91%). Analysis by ^{1}H NMR gave cobalt substitution of ca. 75%.

For **3a**: ^{1}H NMR (400 MHz, THF-d_8, 25 °C) δ 7.54, 7.32 (br s, 5 H, Ph), 4.52, 4.37, 4.29 (br s, 8 H, Cp), 1.12 (br s, Me_{Co}), 0.73 (br s, Me); ^{13}C{^{1}H} NMR (100.5 MHz, THF-d_8, 25°C) δ 201.1 (*C*O), 139.5 (Ph_{Co}),[49] 133.0 (Ph), 131.1 (Ph_{Co}), 129.8 (Ph_{Co}), 129.5 (Ph), 129.0 (Ph_{Co}), 124.4 (Ph), 107.8 (SiC≡*C*Ph), 107.6 (Si*C*C($Co_2(CO)_6$)Ph), 93.5 (Si*C*≡CPh), 81.3 (Si*C*C($Co_2(CO)_6$)Ph), 75.7, 75.1, 74.7, 73.4, 73.0 (Cp), 71.0 (*ipso*-Cp_{Co}), 70.0 (*ipso*-Cp), 2.5 (Me_{Co}), −0.7 (Me); solid-state ^{29}Si NMR δ −5.6 (Si_{Co}), −23.1 ($Si_{no\ Co}$); FTIR (25 °C, Nujol) ν = 2159 (w) (C≡C), 2086 (s), 2048 (s), 2018 (s, br) (CO) cm^{-1}; UV−vis (25 °C, ACS grade THF) λ_{max} = 439 nm, $\epsilon = 9.4 \times 10^2$ L·mol^{-1}·cm^{-1}, Abs. > 0 until ca. 700 nm. Multiple attempts to obtain a satisfactory elemental analysis consistently gave a % C ca. 3% lower than that expected. We attribute this to the formation of a refractory carbonaceous ceramic upon combustion of **Co−PFS 3a**, as this polymer has a ceramic yield of 59% at 900 °C.[22]

Synthesis of Co−PFS 3b. [$Co_2(CO)_8$] (0.025 g, 0.073 mmol) in C_6D_6 (1 mL) was added to a solution of **2b** (0.015 g, 0.048 mmol, $M_n = 6.6 \times 10^5$, PDI = 1.6) in C_6D_6 (2 mL). The reaction mixture was stirred for a further 1 h. The solution changed from light orange to

(46) Ginley, D. S.; Bock, C. R.; Wrighton, M. S. *Inorg. Chim. Acta* **1997**, *23*, 85−94.
(47) Pangborn, A. B.; Giardello, M. A.; Grubbs, R. H.; Rosen, R. K.; Timmers, F. J. *Organometallics* **1996**, *15*, 1518−1520.
(48) Massey, J. A.; Kulbaba, K.; Winnik, M. A.; Manners, I. *J. Polym. Sci. B, Polym. Phys.* **2000**, *38*, 3032−3041.
(49) The subscripts "Co" and "no Co" are used to denote that a particular substituent is bound to an acetylene unit with or without cobalt clusters, respectively. A similar notation is used for Mo−PFS **4** and Ni−PFS **6**.

dark brown, and the release of gas was noted. The solution was precipitated into hexanes through glass wool to remove small amounts of insoluble impurities, and the dark brown precipitate was washed twice with hexanes. All volatile material was removed under high vacuum leaving the dark brown gummy polymer **3b**, with a yield of 0.016 g (64%). Analysis by ^{1}H NMR showed ca. 75% of triple bonds were substituted with cobalt.

For **3b**: ^{1}H NMR (400 MHz, C_6D_6, 25 °C) δ 4.72−4.34 (br m, Cp), 3.00 (br m, CC($Co_2(CO)_6$)CH_2CH$_2$CH$_2$CH$_3$), 2.26 (br m, C≡CCH_2-CH$_2$CH$_2$CH$_3$), 1.71 (br m, CC($Co_2(CO)_6$)CH$_2$CH_2CH_2CH$_3$), 1.60−1.48 (br m, C≡CCH$_2$CH_2CH_2CH$_3$), 1.08 (br m, CC($Co_2(CO)_6$)CH$_2$CH$_2$-CH$_2$CH_3), 0.96 (br m, C≡CCH$_2$CH$_2$CH$_2$CH_3), 0.94 (br s, Me_{Co}), 0.84 (br s, Me); ^{13}C{^{1}H} NMR (100.5 MHz, C_6D_6, 25 °C) δ 200.9 (*C*O), 113.8 (SiC≡*C*Bu), 75.1−72.2 (br m, Si*C*≡CBu, Cp), 35.6 (CC(Co_2-$(CO)_6$)CH$_2$CH$_2$CH$_2$CH$_3$), 35.0 (CC($Co_2(CO)_6$)CH$_2$*C*H$_2$CH$_2$CH$_3$), 31.2 (C≡C*C*H$_2$CH$_2$CH$_2$CH$_3$), 23.1 (CC($Co_2(CO)_6$)CH$_2$CH$_2$*C*H$_2$CH$_3$), 22.4 (C≡CCH$_2$*C*H$_2$CH$_2$CH$_3$), 20.0 (C≡CCH$_2$CH$_2$*C*H$_2$CH$_3$), 14.0 (CC-($Co_2(CO)_6$)CH$_2$CH$_2$CH$_2$*C*H$_3$), 1.6 ($SiMe_{Co}$), −0.2 (SiMe); ^{29}Si{^{1}H} NMR (79.4 MHz, C_6D_6, 25°C) δ −6.5 (Si_{Co}), −25.0 ($Si_{no\ Co}$).

Effect of [$Co_2(CO)_8$] on the Molecular Weight of [Fe(η-$C_5H_4)_2SiMe_2]_n$. [Fe(η-$C_5H_4)_2SiMe_2]_n$ (182 mg, 0.75 mmol, M_n = 38 300, M_w = 79 800, PDI = 2.09) was treated with [$Co_2(CO)_8$] (282 mg, 0.82 mmol) under the conditions described for the synthesis of **3a**. After workup, GPC analysis (conventional calibration) of the polymer gave M_n = 31 700, M_w = 73 500, PDI = 2.32.

Synthesis of Mo−PFS 4. 2a (198 mg, 0.60 mmol, M_w = 2.4 × 10^5, PDI = 2.26) and [{MoCp$(CO)_2$}$_2$] (269 mg, 0.62 mmol) were dissolved in toluene (20 mL), and the dark red solution was heated at 75 °C for 21.5 h. The reaction mixture was cooled to 25 °C, concentrated to $^2/_3$ of its original volume, and precipitated dropwise via a filter cannula into rapidly stirred ACS grade MeOH (250 mL) to give a dark brown precipitate. The solid was washed twice with ACS grade MeOH and once with ACS grade hexanes. Removal of solvent in vacuo afforded a dark brown powder **4**, with a yield of 188 mg (49%). Analysis by ^{1}H NMR showed ca. 69% of triple bonds were substituted with molybdenum.

For **4**: ^{1}H NMR (300 MHz, THF-d_8, 25 °C) δ 7.60 (br s, Ph), 7.34 (br s, Ph), 7.06 (br s, Ph), 6.93 (br s, Ph), 5.04 (br s, Cp_{Mo}), 4.71 (br s, Cp_{Fe}), 4.51−4.27 (m, Cp_{Fe}), 1.29−1.20 (m, Me_{Mo}), 0.89−0.75 (m, $Me_{no\ Mo}$); ^{13}C{^{1}H} NMR (100.5 MHz, THF-d_8, 25 °C) δ 232.8 (*C*O), 231.6 (*C*O), 147.6 (Ph_{Mo}), 133.1 ($Ph_{no\ Mo}$), 131.2 (Ph_{Mo}), 129.9, 129.6 ($Ph_{no\ Mo}$), 128.2 (Ph_{Mo}), 126.6 (*ipso*-Ph_{Mo}), 124.3 (*ipso*-$Ph_{no\ Mo}$), 116.1 (SiC*C*($Mo_2Cp_2(CO)_4$)Ph), 107.5 (SiC≡*C*Ph), 93.5 (Cp_{Mo}), 76.8, 76.1, 74.8, 73.6, 72.7 (Cp_{Fe}), 69.7 (*ipso*-Cp_{Fe}), 4.5 (Me_{Mo}), −0.4 ($Me_{no\ Mo}$); solid-state ^{29}Si NMR (79.3 MHz, spin rate = 4 kHz, 25 °C) δ 0.4 (Si_{Mo}), −22.9 ($Si_{no\ Mo}$); FTIR (25 °C, CH_2Cl_2) ν(CO) = 1983 (m), 1918 (s), 1830 (w) cm^{-1}; GPC (triple detection) M_n = 3.6 × 10^5, M_w = 5.4 × 10^5, PDI = 1.49; UV−vis (25 °C, ACS grade THF) λ_{max} = 557 nm, Abs. > 0 until ca. 700 nm. Anal. Calcd (assuming 69% substitution): C, 54.72; H, 3.67. Found: C, 54.54; H, 3.85.

Synthesis of 5. 1a (299 mg, 0.91 mmol) and [{NiCp$(CO)\}_2$] (333 mg, 1.10 mmol) were dissolved in toluene (6 mL) to give a dark red solution in a Schlenk tube. The tube was placed next to a Philips 125 W mercury lamp, and the setup was wrapped in aluminum foil. The solution was photolyzed for 5 h while vented to an oil bubbler to release evolved CO. The solution became warm to the touch and turned dark green. The solvent was removed in vacuo to give a dark green residue. Recrystallization from toluene/hexanes (3:2) at −35 °C gave a dark green solid, with a yield of 230 mg (44%). Crystals suitable for X-ray crystallography studies were obtained by slow evaporation of a hexanes/CH_2Cl_2 (4:1) solution at 25 °C.

For **5**: ^{1}H NMR (400 MHz, C_6D_6, 25 °C) δ 7.83 (dd, $^3J_{HH}$ = 8.2 Hz, $^4J_{HH}$ = 1.4 Hz, 2 H, *ortho*-Ph), 7.13−7.09 (m, 3 H, *meta*- and *para*-Ph), 5.23 (s, 10 H, Cp_{Ni}), 4.44 (m, 4 H, Cp_{Fe}), 4.34 (m, 2 H, Cp_{Fe}), 4.08 (m, 2 H, Cp_{Fe}), 0.81 (s, 3 H, Me); ^{13}C{^{1}H} NMR (100.5 MHz, C_6D_6, 25 °C) δ 139.4, 131.2, 128.5 (Ph), 127.7 (*ipso*-Ph), 114.6 (SiC*C*(Ni_2Cp_2)Ph), 87.9 (Cp_{Ni}), 86.5 (Si*C*C(Ni_2Cp_2)Ph), 78.0, 77.7, 76.5, 75.5 (Cp_{Fe}), 34.7 (*ipso*-Cp), −0.9 (Me); ^{29}Si{^{1}H} NMR (79.4 MHz, C_6D_6, 25 °C) δ −18.1; MS (EI, 70 eV) *m*/*z* (%) 574 (1) [M]$^+$, 481 (100); HRMS (EI, 70 eV) calcd for $C_{29}H_{26}{}^{56}FeNi_2Si$ 573.986 013, found 573.985 130, fit 1.5 ppm. Anal. Calcd for $C_{29}H_{26}FeNi_2Si$: C, 60.49; H, 4.55. Found: C, 61.46; H, 4.62.

Synthesis of Ni−PFS 6. OMePh$_2$Si-capped **2a** (103 mg, 0.31 mmol, M_n = 4700, PDI = 2.57) and [{NiCp$(CO)\}_2$] (94 mg, 0.31 mmol) were dissolved in toluene (4 mL) to give a dark red solution in a Schlenk tube. The tube was placed next to a Philips 125 W mercury lamp, and the setup was wrapped in aluminum foil. The solution was photolyzed for 4 h while vented to an oil bubbler to release evolved CO. The solution became warm to the touch and turned dark green. After the mixture was cooled to 25 °C, the solution was precipitated via a filter cannula into rapidly stirred hexanes (30 mL) to give a green solid. It was washed multiple times with hexanes until the supernatant was light yellow. The solid was dried in vacuo to give a green powder, with a yield of 117 mg (73%). Analysis by ^{1}H NMR showed ca. 75% of triple bonds were substituted with nickel.

For **6**: ^{1}H NMR (400 MHz, C_6D_6, 25 °C) δ 7.84−7.58 (br, *ortho*-Ph_{Ni} and *ortho*-$Ph_{no\ Ni}$), 7.32−6.96 (br, *meta*- and *para*-Ph_{Ni} and *meta*- and *para*-$Ph_{no\ Ni}$), 5.20 (br s, NiCp), 4.70−4.20 (br m, Cp_{Fe}), 3.55 (br s, SiOMe), 1.09 (br s, Me_{Ni}), 0.86 (br s, $Me_{no\ Ni}$); ^{13}C{^{1}H} NMR (100.5 MHz, C_6D_6, 25 °C) [resonances for acetylenic and methyl carbons in repeat units without Ni clusters were too weak and not discernible from the baseline] δ 140.1, 135.5 (Ph_{Ni}), 132.3 ($Ph_{no\ Ni}$), 131.0 (Ph_{Ni}), 130.2 (*ipso*-Ph_{Ni}), 128.8 ($Ph_{no\ Ni}$), 127.4 (Si*C*C(NiCp)$_2$Ph), 123.7 (*ipso*-$Ph_{no\ Ni}$), 114.2 (Si*C*C(NiCp)$_2$Ph), 88.0 (NiCp), 75.2−73.8, 72.8−71.4 (m, Cp_{Ni} and $Cp_{no\ Ni}$), 68.9 (*ipso*-Cp_{Ni}), 1.9 (Me_{Ni}); ^{29}Si{^{1}H} NMR (79.4 MHz, C_6D_6, 25 °C) [the resonance for silicon atoms in repeat units without Ni clusters was not observed] δ −13.2; GPC (conventional calibration) M_n = 7100, M_w = 13 600, PDI = 1.91; UV−vis (25 °C, ACS grade THF) λ_{max} = 461 nm (less intense peak at λ = 682 nm). Anal. Calcd (assuming 75% substitution): C, 61.93; H, 4.61. Found: C, 61.82; H, 4.83.

X-ray Crystallography. Selected crystal, data collection, and refinement parameters for **5** are given in Table 1. Single X-ray diffraction data were collected at 150(1) K using a Nonius Kappa-CCD diffractometer and monochromated Mo Kα radiation (λ = 0.71073 Å). The data were integrated and scaled using the Denzo-SMN package.[50] The SHELXTL/PC package was used to solve and refine the structures.[51] Refinement was by full-matrix least-squares on F^2 using all data (negative intensities included). Hydrogen atoms were placed in calculated positions and included in the refinement in riding-motion approximation.

CCDC-253896 (**5**) contains the supplementary crystallographic data for this paper. This file can be obtained free of charge via the Internet at www.ccdc.cam.ac.uk/conts/retrieving.html (or from the Cambridge Crystallographic Data Centre, 12 Union Road, Cambridge CB2 1EZ, U.K.).

Substrate Preparation. Silicon (100) substrates were purchased from Wafer World Inc. and cleaned by sonication for 10 min each in ACS grade CH_2Cl_2, ACS grade 2-propanol, piranha solution (30% H_2O_2/concentrated H_2SO_4, 1:3 v/v, CAUTION), and deionized water prior to drying in a jet of filtered air.

Electron-Beam Lithography. The e-beam lithography system was a converted thermionic DSM 940 (Zeiss) scanning electron microscope. The system had been converted by implementing an electrostatic beam blanker and a low hysteresis beam scanning coil. Exposures were carried out at 25 °C on a stage without temperature control capabilities in a vacuum of 10^{-5} Torr or better. A remote computer (PC), using a fast IEEE interface drove the beam and the system stage motor through the Raith Elphy-Plus Pattern generator (32 bits architecture). The system

(50) Otwinowski, Z.; Minor, W. *Methods Enzymol.* **1997**, *276*, 307−326.
(51) Sheldrick, G. M. *SHElXTL/PC*, version 5.1; Bruker Analytical X-ray Systems: Madison, WI, 1997.

Table 1. Selected Crystal, Data Collection, and Refinement Parameters for **5**

	5
formula	$C_{29}H_{26}FeNi_2Si$
M_r	575.86
crystal system	orthorhombic
space group	*Pca*21
color	dark green
a, Å	14.2770(2)
b, Å	9.3405(4)
c, Å	17.8241(5)
α, deg	90
β, deg	90
γ, deg	90
V, Å^3	2376.92(13)
temperature, K	150(1)
Z	4
ρ_{calc}, g cm^{-3}	1.609
μ(Mo Kα), mm^{-1}	2.236
F(000)	1184
crystal size, mm^3	0.20 × 0.12 × 0.08
θ range, deg	2.61−27.48
reflns collected	11811
independent reflns	4720 (R_{int} = 0.0458)
abs. correction	semiempirical from equivalents
max and min transmission coeff.	0.837 and 0.787
parameters refined	299
GoF on F^2	1.043
R1[a] ($I > 2\sigma(I)$)	0.0347
wR2[b] (all data)	0.0803
peak and hole, e Å^{-3}	0.451 and −0.479

[a] $R1 = \Sigma||F_o| - |F_c||/\Sigma|F_o|$; [b] $wR2 = \{\Sigma[w(F_o^2 - F_c^2)^2]/\Sigma[w(F_o^2)^2]\}^{1/2}$.

stage also has a joystick for manual control, and its position is monitored by a laser interferometer (with 5 nm resolution) and read by the computer. A Faraday cup located on the stage connected to a multimeter allows measurement of the beam current using the remote computer.

Satisfactory results were obtained using an accelerating voltage of 25 kV and currents ranging from 1 to 6 nA with a dose of 25 mC/cm^2 for **Mo−PFS 4** and 20 mC/cm^2 for **Ni−PFS 6**. Lower doses led to poor adhesion of features to the surface following solvent development. The sample was a small silicon wafer (1 cm^2) with a 215 ± 5 nm thick **Mo−PFS 4** layer or a 193 ± 5 nm thick **Ni−PFS 6** layer (determined by ellipsometry); it was developed by 2 min (**Mo−PFS 4**) or 12 min (**Ni−PFS 6**) sonication in ACS grade THF. For **Mo−PFS 4**, the selected pattern was an array of bars (0.5 × 4.0 μm^2) spaced 2.0 μm apart horizontally and 3.0 μm apart vertically such that a 100 × 100 μm^2 area contained 560 bars. For **Ni−PFS 6**, the selected pattern was an array of dots (diameter = 1.0 μm) spaced 3.0 μm apart horizontally and vertically such that a 100 × 100 μm^2 area contained 289 dots.

Optical Microscopy. Bright field optical micrographs were obtained using an Olympus BX41 optical microscope equipped with a Pixelink PL-A642 camera and Pixelink capture software.

Scanning Electron Microscopy (SEM). SEM images were recorded using a Hitachi S-5200 field-emission electron microscope.

Ellipsometry. This technique was used as previously described.[37]

UV−Photolithography. Thin films of **Mo−PFS 4** and **Ni−PFS 6** were spin-coated onto cleaned silicon substrates from chlorobenzene and toluene solutions, respectively. The film thickness was determined by ellipsometry: 198 ± 5 nm for **Mo−PFS 4** and 215 ± 5 nm for **Ni−PFS 6**. Each film was exposed to UV light from a 450 W Optical Associates Inc. near-UV mercury lamp (λ = 350−400 nm, actual power = 420 W) through a chrome contact mask for 6 min. After exposure, the pattern was developed by hand agitation of the substrate in ACS grade THF for 2 min.

Acknowledgment. We acknowledge NSERC postgraduate scholarships (for W.Y.C. and A.B.), and an NSERC PDF (for S.B.C.). I.M. and H.E.R. are grateful to the NSERC AGENO program for supporting this research, and I.M. thanks the Canadian Government for a Canada Research Chair. H.E.R. and S.A. thank NSERC, MMO, CITO, ORDCT, and CIPI. We thank Dr. Neil Coombs and Dr. Marc Mamak for assistance with electron microscopy imaging at the Centre of Nanostructure Imaging, Department of Chemistry, University of Toronto, funded by the Canada Foundation for Innovation/Ontario Innovation Trust.

Supporting Information Available: CIF file for **5**. This material is available free of charge via the Internet at http://pubs.acs.org.

JA045386I